Astronomy & Astrophysics manuscript no. 5399pelt
September 14, 2006

Kinematic frames and "active longitudes": does the Sun have a face?

J. Pelt[1], J.M. Brooke[2,3], M.J. Korpi[4], and I. Tuominen[4]

[1] Tartu Observatory, 61602 Tõravere, Estonia
[2] Manchester Computing, University of Manchester, Oxford Road, Manchester, M13 9PL, UK
[3] School of Computer Science, University of Manchester, Oxford Road, Manchester, M13 9PL, UK
[4] Observatory, PO Box 14, FI-00014 University of Helsinki, Finland

Received —; accepted —

ABSTRACT

Context. It has recently been claimed that analysis of Greenwich sunspot data over 120 years reveals that sunspot activity clusters around two longitudes separated by 180°("active longitudes") with clearly defined differential rotation during activity cycles. In previous work we demonstrated that such effects can be observed in synthetic data without such features, as an artefact of the method of analysis.

Aims. In the present work we extend this critical examination of methodology to the actual Greenwich sunspot data and also consider newly proposed methods of analysis claiming to confirm the original identification of active longitudes.

Methods. We performed fits of different kinematic frames onto the actual sunspot data. Firstly, a cell-counting statistic was used to analyse a comoving system of frames and show that such frames extract useful information from the data. Secondly, to check the claim of century-scale persistent active longitudes in a contramoving frame system, we made a comprehensive exploration of parameter space following the original methodology as closely as possible.

Results. Our analysis revealed that values obtained for the parameters of differential rotation are not stable across different methods of analysis proposed to track persistent active longitudes. Also, despite a very thorough search in parameter space, we were unable to reproduce results claiming to reveal the century-persistent active longitudes. Previous parameter space exploration has been restricted to frames whose latitudinal profile is opposite to solar surface differential rotation. Relaxing this restriction we found that the highest values of nonaxisymmetry occur for frames comoving with the solar surface flow. Further analysis indicates that even these solutions are the result of purely statistical fluctuations.

Conclusions. We can therefore say that strong and well substantiated evidence for an essential and century-scale persistent nonaxisymmetry in the sunspot distribution does not exist.

Key words. Sun: activity – Sun: magnetic fields – sunspots – methods: statistical

1. Introduction

1.1. Nonaxisymmetry in late-type stars

It is known that solar active regions may exist at the same position (such as recurrent sunspot groups) during several solar rotations, a new active region appearing at another position (e.g. Tuominen & Virtanen 1987, Pulkkinen & Tuominen 1998). The sunspots reflect intense concentrations of magnetic field and thus occur only at certain discrete locations on the solar surface. For related discussion on the observed magnetogram recordings of the full-disk field see e.g. Stenflo 1991. Consequently, different activity indicators tend to be statistically correlated for a long time spans and a statistical analysis of the corresponding phase distributions must take this into account.

The theory of the global magnetic field (mean-field dynamo theory) has been developed over the last 50 years, starting from a linear theory (Parker 1955, Steenbeck & Krause 1969, for a detailed review see Krause and Rädler 1980), followed by a nonlinear one, where the stability of the solutions determines the symmetry properties of the field (Krause & Meinel 1988, Brandenburg et al. 1989), and including a nonaxisymmetric solution as a possibility in the case of rapid rotation (e.g Rädler et al. 1990, Moss, Tuominen & Brandenburg 1991). More recent models including hydrodynamics show that when the rotation velocity increases, the field geometry changes from antisymmetric with respect to the equatorial plane and axisymmmetric with respect to the longitude, to nonaxisymmetric with respect to the longitude (e.g. Tuominen et al. 1999, Tuominen, Berdyugina & Korpi 2002).

Send offprint requests to: J. Pelt

Recently it has been claimed that long-term, i.e. persistent for at least 120 years, nonaxisymmetric structures can be detected in the solar sunspot data using new methods of analysis that take into account the possibility that such structures follow the differential surface rotation. This is an important claim and in the present paper we investigate it in detail because the existence of persistent "active longitudes" (nonaxisymmetric structures) in old slowly rotating late-type stars, such as the Sun, has important theoretical implications.

1.2. Nonaxisymmetry in solar data

Berdyugina & Usoskin 2003 (hence BU) analysed the longitudinal distribution of regions of sunspot formation in the Greenwich sunspot data for a period of 120 years. By applying phase corrections, corresponding to the differential rotation of regions of activity formation, they claimed to identify persistent (during 120 years) active longitude belts which are separated by 180° and which drift smoothly along longitudes. The essence of their method is to apply a longitude shift correction for each Carrington rotation to represent a different rotation velocity for the active longitudes as the sunspot activity wave moves from high to low latitudes in each solar cycle. As a response to the first paper (BU) Pelt, Tuominen & Brooke 2005 (PTB) demonstrated that large part (or all) of the persistent smooth migration of the active longitudes can be the result of a particular method of data treatment in BU. Essentially it was shown that diagrams, similar to these used as a proof in BU, can be obtained even from random data. The criticisms of the paper were not directed at the observation that there can be active longitudes which persist over time, but towards the claim that such longitudes maintain consistent migration on a century time-scale.

In recent papers Usoskin, Berdyugina & Poutanen 2005 (UBP) and Berdyugina et al. 2006 (BMSU) responded to this critique with the claim that they can confirm the original BU results using much simpler constructions which do not use the data processing methods criticized in PTB. In particular they consider that the new analysis confirms that the active longitudes maintain consistent smooth migration throughout the 120 year period of the sunspot data analysed. The fact that this result was produced by two different methods of analysis of the data is considered to confirm the reality of the phenomenon.

As will be discussed in length below, the migration models given in the first paper (BU) significantly differ from those obtained as a result of the analysis in UBP and represented in the data analysis part of BMSU. This is most readily seen in the cumulative frame kinematics: the BU frame makes about 28 extra rotations compared to the Carrington frame, contrasted with the UBP values of about ≈ 11 rotations for the Northern hemisphere and about ≈ 14 for the Southern hemisphere. The particular key feature here is that in BU the Northern and Southern frames keep coherently in phase whereas in UBP the Southern frame lags with respect to the Northern one. This indicates the need for a very thorough analysis of the methods of analysis used in constructing the differentially rotating frames considered to "freeze" the longitudes of these nonaxisymmetic features.

This paper is structured as follows: in section 2 we describe the data and the background to our analysis. In section 3 we demonstrate that kinematic frames which follow the rotation of sunpots exist and can clarify the basic properties of the longitudinal distribution of sunspots. In section 4 we present an examination of parameter space using the methods used in UBP but increasing the resolution and the range of the parameter space search. In section 5 we discuss these results and introduce clarificatory statistical computations to check whether bimodal distributions could be statistical fluctuations. Finally section 6 presents our conclusions.

2. Data and methods of analysis

2.1. Details of datasets analysed

Our input data for statistical analysis was downloaded from the same Science at NASA web site[1] as in BU and UBP. The format description supplied with the data sets turned out to be incomplete and to unscramble the data we used the original document from NOAA Satellite and Information Service Site[2]. During the data checking we found some outliers in the data. The record from observations of year 1980 which referred to longitude 408.9° was rejected and for couple of records where longitude was only slightly more than 360° we subtracted 360° from the given value (assuming circularity). The subset for years 1878-1996 was then singled out to be compatible with papers under scrutiny. In the terms of Carrington rotations we used rotations 325-1917 for both hemispheres. For each particular sunspot group or single spot we selected only the record of its first occurence as was done in original papers. It is important to note that some sunspot group numbers in data base are multiply used. To count them as separate entities we used the index value from the 21st column in the records (this was the piece of information missing in the first format description mentioned above). Finally we had two data sets: 1593 rotations and 18680 records for the Northern hemisphere and 1593 rotations and 17966 records for the Southern hemisphere; the compiled data sets are available on the web[3]. In the original papers "about 1600" rotations and "about 40000" records were used.

To simplify the discussions below we will often renumber the original Carrington rotation numbers in our data set to start from 1 (hence $1, \ldots, 1593$). Furthermore, in all the plots and formulae we adopt the basic phase interval

[1] http://science.msfc.nasa.gov/ssl/pad/solar/greenwch.htm
[2] ftp://ftp.ngdc.noaa.gov/STP/SOLAR_DATA/SUNSPOT_REGIONS/GREENWICH/GROUPS/format.grp
[3] http://www.aai.ee/~pelt/soft.htm

$0° - 360°$. As a result, some formulae can differ from those of the original papers. However, the original forms can easily be recovered by using an appropriate phase shift.

2.2. Construction of kinematic frames for analysis

Two different physical scenarios can be considered when thinking of how to construct a framesystem. If one is to construct a frame to correct for the solar surface differential rotation, it is natural to construct a frame that is moving with this flow. To investigate the situation where a rigidly rotating nonaxisymmetric structure anchored to the solar core would "illuminate" the solar activity belt influenced by differential rotation (the stroboscopic explanation discussed by BMSU), a more natural starting point would be to investigate frames which move against the solar surface differential rotation pattern. As both situations could occur in the Sun, neither of them should be excluded from the analysis.

Let us now divide the full set of sunspot records into a set of subintervals of length 27.2753 days, the Carrington rotation, as proposed originally by BU. For each particular rotation $i, i = 1, \ldots, N$ (where N is the total number of rotations in the set) the local phase shift Ω_i is defined (in degrees per day). It can be constant or depend on a mean latitude of sunspot formation and free parameter B as in Eq. 6. If the frame is to follow the differential rotation pattern then, over the full time span, the shifts accumulate according to the formula

$$\Lambda_i = \Lambda_0 + T_C \sum_{j=1}^{i} (\Omega_j - \Omega_C), \quad (1)$$

i.e. the frame will lag if the sunspots rotate slower and will be advanced for more rapid rotation. Here $T_C = 25.38$, $\Omega_C = 360°/T_C$ and Λ_0 is a general phase shift to be computed later. Hereafter we refer to this frame system as the *comoving* frame. The other possibility is to choose a system of frames that moves in the opposite direction if compared to the surface rotation pattern, when the shifts are defined as

$$\Lambda_i = \Lambda_0 + T_C \sum_{j=1}^{i} (\Omega_C - \Omega_j). \quad (2)$$

We will refer to this frame system as the *contramoving* frame.

If the differential rotation is defined as Eq. 6, then we see that for the comoving frame, positive values of B lead to phases being pushed backwards if sunspots occur at higher latitudes where they rotate slower. If we allow for negative values of B, in the comoving frame they correspond to frames that are pushed forward with slower rotation. The opposite sign rule applies for the contramoving frames, positive Bs lead to phases being pushed forward with slow rotation and negative Bs to a situation where the frame follows solar-type differential rotation. The basic difference of the two frame systems is illustrated in Fig.4; the comoving frame phase shift curve resulting from the best solution from the cell-counting statistics presented in Sect. 3 is plotted with a thin solid line and the original UBP Northern contramoving solution phase shift on top of it with a thick solid line. In the former solution the positive B-value causes the phases to lag behind during the early stages of the solar cycle (sunspots at higher latitudes) whereas the positive value in the latter solution results in phases being pushed forward during the early stages.

If we do not restrict the parameter Ω_0 and allow for both positive and negative values of the parameter B within each frame system, one can see that formally the two types of frames are equivalent, and both types of physical situations of interest are detectable by both methods. In this study we utilise both types of frames with no restriction on the sign of B. We note here that in UBP and BMSU the analysis was restricted to the contramoving formulation with positive B values only. It is a key point that, as we demonstrate below, although formally equivalent, they are not statistically equivalent. This is due both to the interaction of the frames with random fluctations in longitudinal distributions and also to the method of analysis proposed in UBP.

To facilitate the comparison and transformation between the framesystems, the contramoving parameters translate to comoving frame by the following formulae

$$B^{comov} = -B^{contra} \quad (3)$$

$$\Omega_0^{comov} = 2\Omega_C - \Omega_0^{contra}. \quad (4)$$

Here we also note that special attention is needed when contramoving rotation laws are plotted together with comoving rotation laws (e.g. observational data from sunspots or helioseismology). The contramoving parameters must first be translated to comoving frame by the formulae given above. For instance, the best frame for the Northern hemisphere in UBP, obtained in the contramoving formulation with the parameters Ω_0^{contra}=14.33 and B^{contra}=3.40, translates to comoving parameters Ω_0^{comov}=14.05 and B^{comov}= -3.40, i.e. slow rotation at the equator which cyclically speeds up as a function of latitude. We have illustrated the possible error related to treating the comoving and contramoving frames as equals in our Fig. 5, where we have plotted the best Northern UBP frame twice: the thin solid line represents the original illustration of UBP where the rotation law with the contramoving parameterization is plotted amongst comoving rotation laws without transformation. With the solid thick line we plot the transformed UBP rotation law in the comoving frame. Here it can be clearly seen that comparisons of the UBP results with the solar surface differential rotation indicators are not meaningful.

3. Cell-counting method

To illustrate how the kinematic frames work in practice, in this section we construct and analyse one frame system

with a statistical method that is as simple as possible. We choose the comoving formulation, for which the phase shift is defined as Eq. 1. Next we subtract the flow model from actual longitudes

$$\tilde{\lambda}_{ki} = \lambda_{ki} - \Lambda_i - m_{ki} \times 360^\circ, \quad (5)$$

and select integers m_{ki} so that the results will lay in the interval $[0, 360^\circ]$. As we now work in the comoving formulation, after the subtraction we get a certain distribution of longitudes in a frame which is at rest with respect to the differential rotation pattern.

Our comoving frame, as any other frame model in general, depends on a set of parameters (typically Ω_0, B and Λ_0). For each set of parameters we can compute corrected phases λ_{ki} (see Eq. 5) and a value of a certain merit function (criterion) which characterizes distribution of these phases (longitudes). For compatibility we will use merit functions whose parameter dependent *minima* are indicators of the desired types of phase distributions.

To define our first merit fuction we divide all Carrington rotations into groups of ten rotations and all longitudes (phases) into 6° wide cells. We work with 1593 separate rotations altogether and thus get a matrix of 60×160 cells. For each set of free parameters (here Λ_0 and Ω_0) we compute a merit function in the following simple way: Each of the corrected phases $\tilde{\lambda}_{ki}$ belongs to a certain cell. Some of the cells remain empty because there are no sunspots in this particular rotation and interval of phases. As a criterion we use the ratio of occupied cells to the total number of phases. The rationale of this scheme is to produce a measure that is sensitive to the potential existence of longitudes of enhanced spot formation. If the spots or spot groups form at persistent longitudes (in a corresponding frame), they tend to have their first observation in the cells which contain or are close to this persistent longitude. By fixing the cell length in number of rotations, we also fix the length of time interval for which we assume the activity to be persistent. The width of the cells fixes the amount of allowed phase dispersion during this number of rotations.

3.1. Comoving frames with fixed angular velocity

We now demonstrate that the formalism just described is sound and usable. We start from the simplest system of shifts $\Omega_i = \Omega_0$, that is, we assign a constant shift Ω_0 for each Carrington rotation. We let Ω_0 vary in a wide range around the Carrington rotation velocity Ω_C, and calculate the simple cell-counting merit function described above as function of Ω_0; this is depicted in Fig. 1. The dependence on Λ_0 is "minimized out". The curve is somewhat noisy, but still demonstrates clearly how the phases start to line up for Ω_0 values larger than ≈ 14.1 deg/day and how the merit function value again increases from approximately 14.6 degrees per day. The wide depression is too noisy to single out an optimal frame for all latitudes together.

We now generalize our method to accomodate differential rotation by preselecting latitudinal strips and repeating the analysis on each of these subsets separately. We see from Fig. 2 that the minima for each subset are more clearly defined and show a shift representing the migration between latitudes with different rotation velosities. The values of Ω_0 for different strips can be used to build a latitudinally dependent rotation profile. The equatorial angular velocity is ≈ 14.37, for middle latitudes ≈ 14.18 and for high latitudes ≈ 13.40 degrees per day. The merit function curves are still noisy, but they can be improved by smoothing. Because of the different amount of activity indicators in different latitude strips the general level and scatter for the three curves are different. By constructing this merit function we can show that

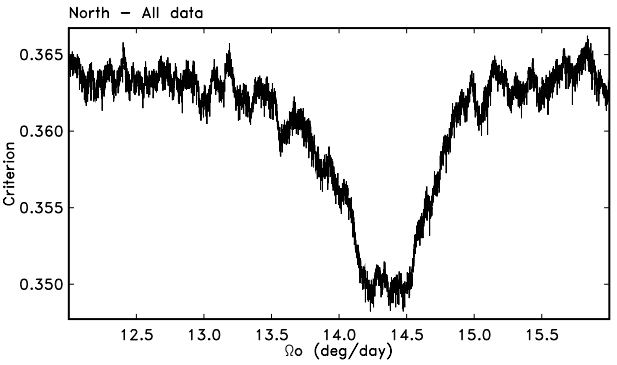

Fig. 1. The cell-counting merit function plotted against Ω_0 for the comoving frame with fixed angular velocity.

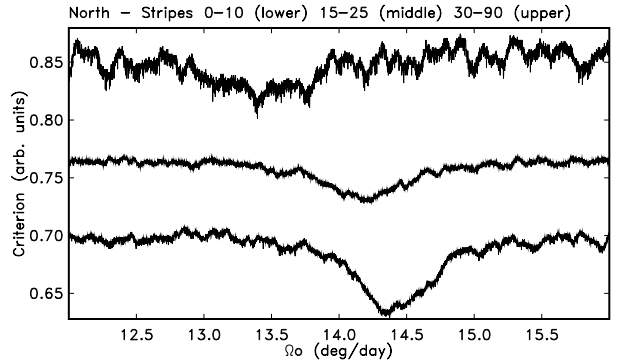

Fig. 2. Merit functions for the subsets of data in different latitude strips. The minima are now shifted and this is a result of differential rotation.

- The hypothesis of comoving frames shows the existence of a range of preferred frames even when applied to the full 120 year data set.
- The scheme with phase corrections allows the computation of optimal parameters for different comoving frames.
- The comoving frames in different latitude strips have stable rotational velocities revealed as principal merit function minima.

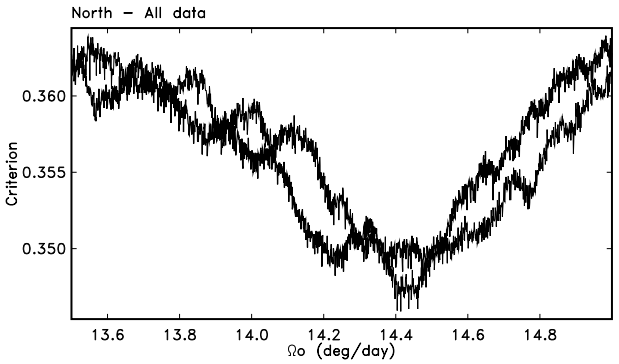

Fig. 3. Merit functions computed for the whole data set: $B = 0$ (fixed angular velocity, thick line), $B = 2.32$ (varying angular velocity, thin line).

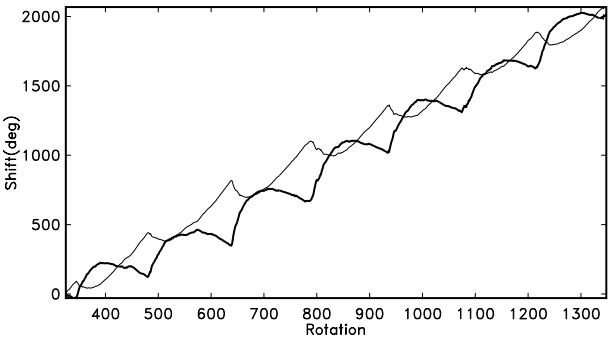

Fig. 4. Typical shift curves for comoving (thin line) and contramoving (thick line) frames.

– The minima of the merit functions are located inside wide depressions, which shows that they are not minor fluctuations manifesting themselves as narrow peaks.
– The kinematics of frames corresponds to kinematics of differential rotation - frames at higher latitudes tend to rotate slower than frames near equator.

In this analysis we have used the longitudes of formation of all sunspots (not weighted by area) since we wish first to test the most basic hypothesis of persistence of activity formation.

3.2. Comoving frames with changing angular velocity

Moving on from the basic analysis above, we now attempt to detect an optimal single frame for all latitudes including weighting for sunspot area. Following UBP we will now include an additional term for each Carrington rotation:

$$\Omega_i = \Omega_0 - B \sin^2\langle\psi\rangle_i, \tag{6}$$

where $\langle\psi_i\rangle_i$ is an area weighted average latitude for i-th Carrington rotation and parameter B measures the amplitude of the latitude dependent part.

To get the optimal triple of frame parameters we need to compute merit functions for a large grid of trials. Using a two step procedure, decribed in detail below, we found a global minimum for the parameter grid $(\Omega_0 \times \Lambda_0 \times B) = [13.5 - 15.0; 0.001] \times [0.0 - 6.0; 0.02] \times [1 - 5; 1]$[4] to be located at $\Omega_0 \approx 14.416$ and $B \approx 2.32$. The range of Λ_0 investigated results from the fact that there are only six different starting positions for 6°-wide cells. The resulting merit functions are depicted in Fig. 3 and the corresponding shifts for the comoving frame in Fig. 4.

It is important to stress that the strongest minimum for the frames with changing angular velocity is deeper compared with that of the fixed angular velocity frames. Consequently it indeed models to some extent real features in the distribution of sunspot longitudes.

This analysis demonstrates that the formalism of comoving frames can reproduce previous results which show that sunspots form at longitudes which can persist for time period much longer than a Carrington rotation.

4. The UBP method

The basic claim of BU, UBP and BMSU is that two preferred longitudes separated by 180° persisting over the last 120 years can be seen in the distribution of sunspot longitudes. These "active longitudes" migrate in any frame with fixed angular velocity, but form coherent and persistent longitudinal structures in a certain frame with changing angular velocity. In the previous section we have shown that frames with changing angular velocity can be used to reveal short-term (of the order of 10 rotations) persistent structures.

The first difference between our simple cell-counting example method and the method of UBP comes from the fact that they have chosen to use phase corrections of the contramoving type, given by Eq.2. The second difference is the usage of sunspot areas. Our simple merit function treats only longitudes whereas the areas are accounted for only when computing the mean latitudes. In UBP the areas are first normalized and then used as weights in the merit function. This amplifies the effect of the spots occurring during the low activity interval of the solar cycle. The third difference is the usage of different merit functions. Since in UBP the authors seek a particular phase distribution they use a particularly crafted bimodal merit function (see Fig. 6 and Eq. 7), whereas ours seeks to minimize phase drift between cells.

Since the claims of UBP go well beyond previous analysis of persistence of nonaxisymmetric features and lead to results which are difficult to explain (e.g. disconnection of Northern and Southern hemispheres) we present a very detailed and careful analysis of the full parameter space below. The only principal difference between our analysis

[4] Here and below we use a systematic notation for computation grids. Inside the square brackets we give minimum and maximum values for the parameter in question followed by the stepsize of computation.

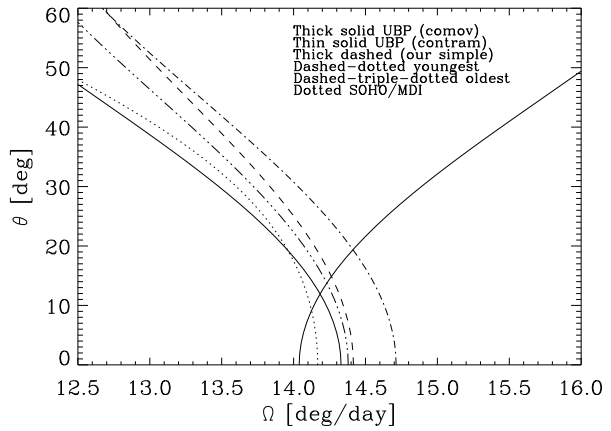

Fig. 5. Comparison of differential rotation curves obtained from helioseismology (SOHO/MDI, Schou et al. 1998), for sunspots of different ages (Pulkkinen & Tuominen 1998), and for the different frame formulations investigated in this paper.

in this section and the UBP investigation is the extension of the method to negative values of B, i.e. we also allow for the possibility to correct for solar-type differential rotation. Otherwise we have followed the original implementation as carefully as possible. The important refinements are given in detail below. Possible reasons why our results differ from those of UBP are given in Sect.5.

4.1. Search for the optimal frame

For every combination of parameters Ω_0, B and Λ_0 we can build a corresponding frame. The shifted phases are then evaluated with the UBP method using the merit function

$$\mathcal{E} = \frac{\sum_i \sum_k A_{ik} \epsilon_{ik}^2}{\sum_i \sum_k A_{ik}}, \tag{7}$$

where $\epsilon_{ik} = \min(\min(\tilde{\lambda}_{ik}, 360^\circ - \tilde{\lambda}_{ik}), |\tilde{\lambda}_{ik} - 180^\circ|)$ measures the distance between the corrected phases and the nearest centre (0° or 180°)[5].

In the actual computations described below we used a phase-shifted version of the merit function, so that the expected maxima in the longitude distribution were shifted to 90° and 270°. This is to ensure uniformity of all the plots.

Thus our absolute phase values differ from UBP, however estimates of bimodality and departure from axisymmetry are clearly unaffected by this shift. In the plots below we depict the merit function values without normalization, this does not affect the interpretation of the plots. In the table 1 we present the true (normalized) values of $\mathcal{E}$.

[5] In the printed version of UBP this function is given incorrectly. This mistake was also confirmed by I. Usoskin, one of the authors of UBP 2005

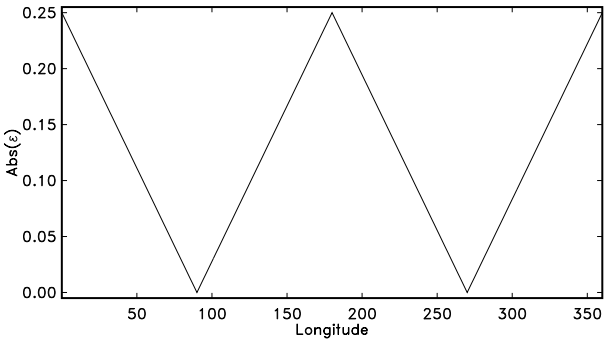

Fig. 6. The merit function depends on the distance of a particular phase from the nearest centre (90° or 270°). It is expected that the distribution sought for will have two maxima, situated 180° from each other.

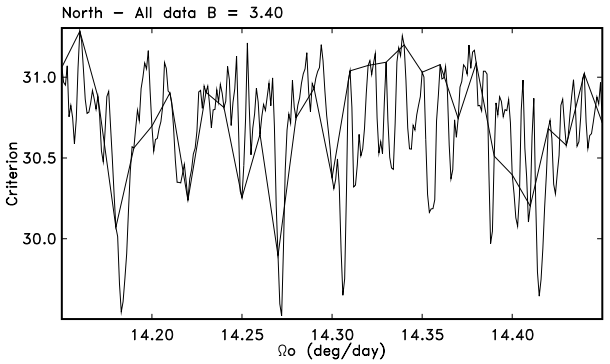

Fig. 7. The merit function dependence on Ω_0 is computed with two different time steps: 0.01 and 0.001.

The dependence of ϵ_{ik}-s on the corrected phases is depicted in Fig. 6. Values of A_{ik} in Eq. 7 are defined as

$$A_{ki} = S_{ki} / \sum_j S_{ji}, \tag{8}$$

where S is the observed spot area corrected for the projection effect, and the sum is taken over all the accounted for spots in the given Carrington rotation.

For each particular triple $(\Lambda_0, \Omega_0\, B)$ we can compute the corresponding shifts and then evaluate the obtained phase (longitude) distributions using the merit function $\mathcal{E}$. Before the actual computations for a full parameter space it is important to estimate the required step lengths along each parameter.

We start from the parameter Ω_0. If we look how the shifted phases depend on changes in this parameter, we see that a small incremental change in the parameter, $\Delta\Omega_0$, is multiplied by the constant $T_C = 25.38$ and then, depending on the particular rotation, by the number of accumulated rotations. For the last phase the number of rotations is approximately 1600.

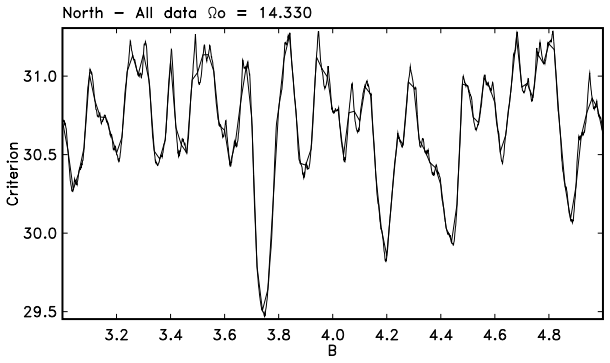

Fig. 8. The merit function dependence on B is computed with two different time steps: 0.02 and 0.001.

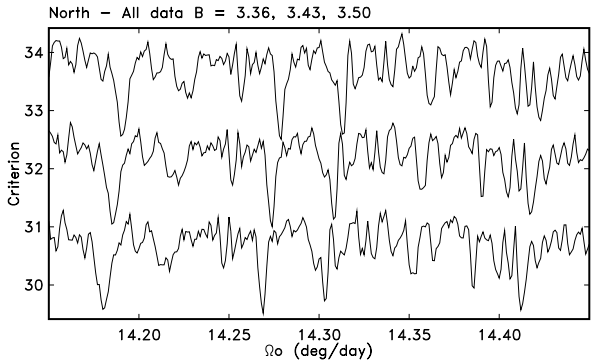

Fig. 9. The merit functions for three different values of B. It is clearly seen that all three are quite similar and only slightly shifted along Ω_0. On a two-dimensional diagram this would look like a row of slanted stripes.

To recover full details of the merit function we fix a certain maximum allowed phase shift for one step change in the input parameter Ω_0. Because there are two increasing and two decreasing parts in the distance function (see Fig. 6), we choose one eighth of the full phase range (45°) as the maximum allowed phase shift. We obtain

$$\Delta\Omega_0 = 45/(T_C * 1600) \approx 0.001. \quad (9)$$

The suitability of this choice is clearly illustrated in Fig. 7 where we plot the merit function running along Ω_0 with two different steplengths: 0.01 (thick curve, the stated precision in UBP) and 0.001 (thin curve). Some important features are certainly lost for the undersampled case. (In this plot and in all the following Ω_0 or B dependent plots, the dependency on Λ_0 has been "minimized out" using the steplength 5°.) For local refinements and for short parameter intervals we have used even smaller values of $\Delta\Omega_0$.

The precise analysis for the B parameter is complicated because of the random component in the mean latitudes. Some simple conclusions can be made by using a trial and error analysis. As seen from Fig. 8 the choice of the step length 0.02 (thick curve, stated precision of B in UBP) is reasonably good, compared with the steplength 0.001 (thin curve). Nevertheless, some minima can be slightly misplaced due to the undersampling. As a compromise, a proper choice for the B stepsize could be 0.002.

The dependence of the merit function on the parameter Λ_0 is obviously smooth and we can use a coarser step in degrees, say 5° to 10°. Because the distance function is periodic with a period 180° we can restrict our search to the subinterval $0° - 180°$.

We can now compute the total number of trial triples we need to work with. Say we want to seek for a global merit function minimum in the parameter space $[10 - 20] \times [0 - 6] \times [0 - 180]$ (according to one of the authors - I. Usoskin (2005), this was exactly the chosen parameter range in their initial search). With the chosen steplengths, we need to evaluate at least $(10 * 1000) * (6 * 500) * 18 = 540000000$ triples. This is far beyond our computational capabilities. Computations with significantly longer steplengths for the parameters would leave us uncertain of recovering the actual global minima. However, we are able to reduce the search space by observing that B and Ω_0 are not completely independent parameters. Observing the similar shapes of curves for different values of B in Fig. 9 and noting the structure of Eqs. 1 and 2, we see that the cumulative shifts depend monotonically on the positive-definite sums

$$S_j = \sum_{j=1}^{i} \sin^2\langle\psi\rangle_j. \quad (10)$$

This component effectively consists of two parts: a wave which models the differential rotation during the solar cycle and a linear part which depends monotonically on the sum of previous waves. In the final cumulative sums the fixed part of this sum is combined with a similar linear component which comes from the parameter Ω_0. Because these contributions are included in the cumulative sums with opposite sign, we can compensate for the increase in the parameter B with the increase in the parameter Ω_0. Their total contribution, which is the difference, then stays fixed. The only change is a small redistribution in phases which comes from the cyclical part.

We can now reparameterize our analysis. First we define a linear part of the curve $S_j, j = 1, \ldots, N$. Then we subtract this linear part from the curve and add it to the Ω_0 dependent part. Finally we will have new parameter Ω_0' which will depend on original Ω_0 and B:

$$\Omega_0' = \Omega_0 - A_C \times B, \quad (11)$$

where $A_C = (S_N - S_1)/(N - 1)$ is the linear slope of the cumulative sum of S_j-s. The new parameter Ω_0' will now describe an overall constant rotation incrementing in phase and the parameter B measures the contribution from the differential rotation. The parameter Ω_0' now describes *the mean comoving framespeed* and the parameter B small phase shifts due to the differential rotation.The effect of reparameterization is clearly seen in Fig. 10, the

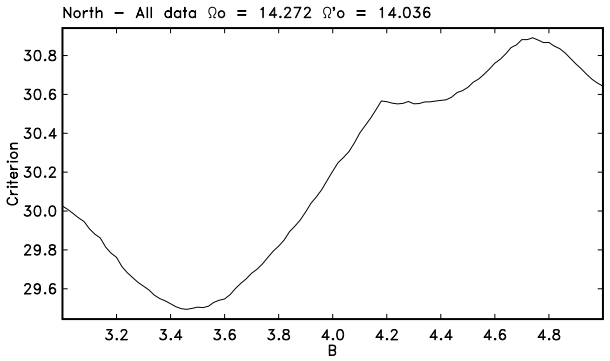

Fig. 10. For the reparameterized case the dependence on B is much smoother (compare with Fig. 8).

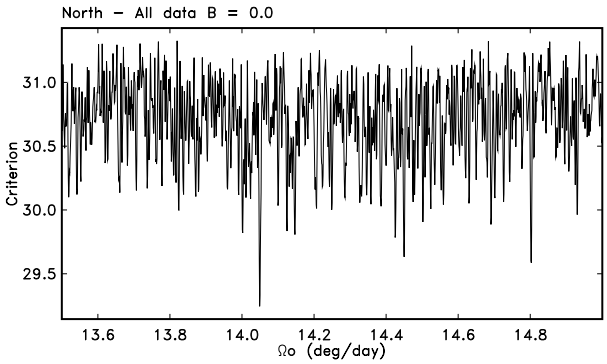

Fig. 11. The merit function computed with $B = 0$ for the Northern hemisphere.

dependence on the parameter B is much smoother and it is possible to decrease the required number of parameter triples. We can now formulate our optimization strategy. First we perform a coarse search using the reparameterized triples. The proper steplengths for this case are 0.001 for Ω_0', 0.1 for B and 5° for Λ_0. The standard Ω_0 can then be computed from Ω_0'. In the vicinity of the detected minima we can perform high resolution refinements using the normal triples of parameters with steplengths 0.0001 for Ω_0, 0.002 for B and 1° for Λ_0.

To characterize the search results and estimate their significance we adopt the measure of nonaxisymmetry defined by UBP. For each distribution of longitudes we form two subsums of corresponding spot areas

$$N_1 = \sum_{k,i} A_{ki}\,, \text{ if } |\tilde{\lambda}_{ki} - 90°| < 45° \text{ or } |\tilde{\lambda}_{ki} - 270°| < 45°,$$
$$N_2 = \sum_{k,i} A_{ki}\,, \text{ otherwise,} \qquad (12)$$

where the summation is taken over all the spots in all the Carrington rotations. The nonaxisymmetry Γ is then defined in UBP as

$$\Gamma = \frac{N_1 - N_2}{N_1 + N_2}. \qquad (13)$$

Non-uniform (in longitude) distributions give higher values of Γ.

4.2. Search results

We restricted our search space for Ω_0 to the interval $[13.5 - 15.0]$ since this includes all the physically plausible values for this parameter. We present our results in three parts. First we give results for fixed angular velocity frames, then for frames with particular values of B and finally for the full parameter space investigated. This allows us to illustrate some important aspects of the merit function "surface".

4.2.1. Fixed angular velocity frames

From the previous discussion we know that it is quite easy to find particular comoving frames for separate latitude strips and even mean frames for the full data. Therefore we first evaluate frames with $B = 0$. From UBP we learn that"...the hypothesis of rotation of the active longitudes with a fixed rate (giving $\Gamma = 0.02 - 0.03$; see Figs. 2a, 3a, and 7a,b) cannot be distinguished from the null hypothesis of the axisymmetric sunspot distribution". Our results of the subset search with $B = 0$ are depicted in Fig. 11 and in table 1. Comparing Fig. 11 with Fig. 1, we observe a key difference: instead of the wide depression we see a number of sharp minima. The strongest peaks are located at ≈ 14.05 for North and ≈ 13.85 for South. The nonaxisymmetry measure is $\Gamma = 0.064$ (North) and $\Gamma = 0.073$ (South), instead of $0.02 - 0.03$ in the original paper. We are dealing here (and also below) with the fluctuations themselves, therefore error bars (e.g. about some mean value) are not relevant.

4.2.2. Frames with fixed values of B

To make straightforward comparisons with the UBP results we sought merit function minima of slices with fixed B values. For the Northern hemisphere we tried to recover the original result in a slice with the best UBP value of $B = 3.40$; for the Southern hemisphere our slice was selected with the best UBP value of $B = 3.39$. The results are given in table 1.

In addition to the computations with positive values of B we computed "spectra" also around their negative counterparts. It is clearly seen from the corresponding tables that our results differ significantly from these presented in UBP. Fig. 12 is of particular significance when compared with Fig. 3, where we can see that the best comoving frame shows itself as a very clear minimum in the middle whose width is much greater than that of the fluctuations. In Fig. 12 we observe only a bunch of narrow fluctuations. With the merit function used in section 3, when we change the parameter values, then in the vicinity of the main min-

Comment	N/S	B^{comov}	Ω_0^{comov}	B^{contra}	Ω_0^{contra}	$\mathcal{E}$	Γ	B^{ubp}	Ω_0^{ubp}	Γ^{ubp}
Fixed B	N	-3.40	14.0971	3.40	14.2717	0.0195	0.059	3.40	14.33	0.11
Fixed B	N	3.40	14.3652	-3.40	14.0036	0.0195	0.064	-	-	-
Fixed B	S	-3.39	13.6344	3.39	14.7344	0.0196	0.038	3.39	14.31	0.09
Fixed B	S	3.39	14.6170	-3.39	13.7518	0.0192	0.070	-	-	-
No diff. rot	N	0	14.3196	0	14.0492	0.0194	0.064	0	?	0.02-0.03
Global search	N	-1.48	14.3183	1.48	14.0505	0.0191	0.079	3.40	14.33	0.11
Global search	N	3.92	14.4395	-3.92	13.9293	0.0190	0.096	-	-	-
No diff. rot	S	0	14.5193	0	13.8495	0.0194	0.073	0	?	0.02-0.03
Global search	S	-0.63	14.4992	0.63	13.8696	0.0191	0.068	3.39	14.31	0.09
Global search	S	3.72	14.6404	-3.72	13.7284	0.0190	0.082	-	-	-

Table 1. Summary of the search results with the UBP method. The analysis is performed in the contramoving formulation: the obtained frame parameters are given in the columns 5 and 6, and transformed into the comoving formulation in columns 3 and 4. The corresponding best values from the original UBP paper, if available, are given in columns 9 and 10.

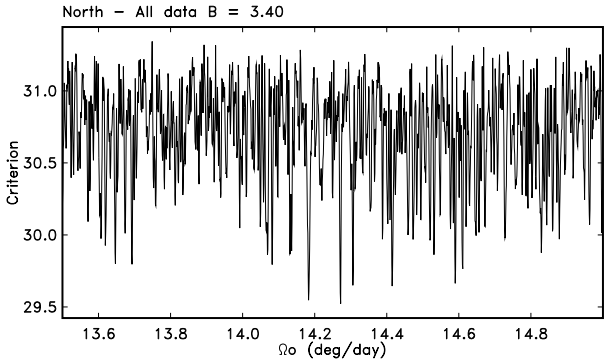

Fig. 12. The merit function computed with $B = 3.40$ for the Northern hemisphere. This figure should be compared with Fig. 3.

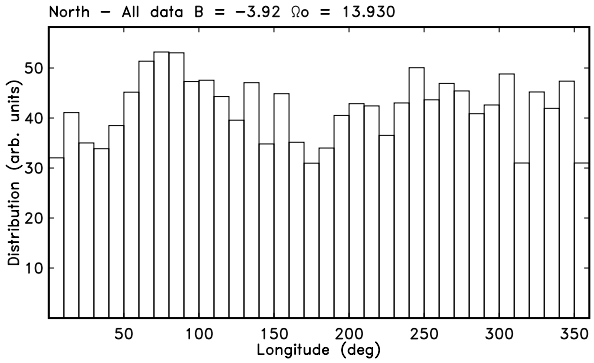

Fig. 13. Strongest fluctuation for Northern hemisphere.

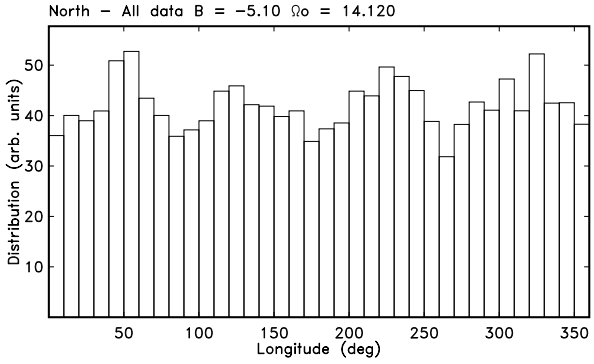

Fig. 14. Longitudinal distribution obtained with best parameter fit for a merit function with four maxima. The parameter space used in the search was the same as in Fig. 13.

imum, phases migrate slowly from one cell to another and the general picture changes slowly. With the UBP merit function (crafted for bimodal waves), we observe a highly fluctuating curve, with no observable minimum of width greater than the fluctuations.

4.2.3. Global search

In the global search we allow B also to vary freely. The results of the global computations are summarized in table 1 and in Fig. 13. The distribution for the Northern hemisphere does not show the clear bimodal structure presented in UBP, but its nonaxisymmetry is quite high - $\Gamma = 0.096$. Our results with the contramoving formulation and UBP merit function show that there are no minima with width greater than the fluctuations which would be expected from causal dependence on the parameters. Given this, we observe that the strongest minima tend to occur for the negative values of B, which translate to solutions with the comoving frame formulation.

Possible reasons for the difference between our results and the results presented in BU and UBP can be:

- The data sets used in UBP and here can be different. The authors of UBP may have used certain pre- or postselection principles applied to the input data (not described in the paper).
- The curves of the mean latitudes (and therefore also the shift frames) in UBP were smoothed in a particular

way (see Fig. 1 in UBP) or were interpolated in a particular way (compare Fig. 5 in BMSU to our Fig. 15). However, we did not find any comments about these procedures in either of the papers.

Below we try to look at some other possibilities. To check if the bimodal merit function gives clearly superior results for departures from axisymmetry, we constructed a merit function with four maxima over the full range of longitude and performed a full parameter space search as above. This represents not two migrating density waves but four, two for each side of the Sun. The fluctuation which gave the global minimum for this criterion is depicted in Fig. 14 (Northern hemisphere). The distribution is certainly non-uniform and four expected waves are clearly seen.

5. Discussion

The results obtained above and those of BU, UBP and BMSU (data analysis part) show discrepancies which require some explanation. Below we present how we tried to control our procedures to discover potential reasons for such major differences. We also include comparative analysis of the results of BU and UBP since a major contention of PTB is that the attempt to detect persistent features of the sunspot data is very sensitive to the methodology used.

5.1. Kinematics of frames

The most significant problem with the persistent longitude strips is connected to their cumulative kinematics.

The authors of BU found that in the Carrington reference frame the observed migration had a phase lag about 2.5 solar rotations per sunspot cycle, in total about 28 rotations during 120 years.

In the follow-up study (PTB) we demonstrated that a major part of this effect can be due to hidden assumptions in the methodology of data processing. In the next paper (UBP) the authors attempt to confirm their original conclusions by constructing a new set of contramoving frames using global optimization techniques. The selected dynamic frames, however, differ significantly between BU and UBP & BMSU: in the former case the pattern makes 28 extra rotations during 120 years, whereas in the latter, the Northern pattern makes ≈ 11 and Southern ≈ 14 rotations. The reader can easily verify this by comparing Figs. 3-4 from BU with Fig. 1 in UBP and especially with Fig. 1 in BMSU, where the different frames and their kinematics are depicted graphically. Consequently we consider that the two latest papers (UBP and BMSU) fail to confirm the results obtained in the first paper (BU), in particular they do not refute the conclusions of PTB.

The second kinematical problem is connected to the different parameterization schemes. In the UBP investigation, a contramoving frame system is used, in addition restricted to positive values of the parameter B. As discussed in length in Sect. 2.2, to construct a frame system comoving with the solar surface differential rotation pattern, negative B values should have been allowed for. Now the solutions are restricted to trace a situation where movement in the opposite direction than the differential rotation pattern occurs. Since we have demonstrated in section 2.2 that these frames are not equivalent methods of treating the observational data, the restriction of positivity of B should be dropped, as in this study. As a consequence, with the UBP method, we find the highest nonaxisymmetry measures for frames with negative Bs, i.e. moving with the solar surface differential rotation pattern.

The third kinematical problem comes from the fact that the numbers of extra rotations (compared with Carrington frame) are in the UBP model significantly different for the Northern and the Southern hemispheres: ≈ 11 and ≈ 14 correspondingly (cf. Fig. 1 in BMSU). This raises serious difficulties for the dynamo theory of the large scale magnetic field.

5.2. Evidence of flip-flops in the dominant longitude

Another important result of BU is the alternation of dominance between the two longitudinal maxima with the approximate periods of 3.8 (North) and 3.65 (South) years (periodicity in flip-flops). The flip-flop phenomenon was originally found in an extremely active late-type star FK Com (see Jetsu, Pelt & Tuominen 1993).

The particular values for the mean flip-flop periods for the Sun (in BU) were obtained from an analysis of the power spectra. Firstly the evidence presented does not establish that such periodicity exists. From the power spectrum plot of Fig. 8-9 (BU) it is clear that *nearly all the spectral power fluctuations* are above the line of 95% confidence level. If there were clear and dominant periodicity one would not expect this.

In UBP it is claimed that the flip-flop events and their periods obtained in BU are valid also for the newly constructed dynamic frames and the resulting coherent nonaxisymmetric structures. The flip-flop event frequency, however, was computed using a frame which rotates nearly three times more rapidly than the dynamic frames found in UBP. We note that a phase shift of $\approx 180°$ which causes the flip-flop event position to swap longitude can be produced by 0.004 degrees per day change in the frame model parameter Ω_0 (quoted precision in UBP for this parameter is 0.01). In the new construction, in addition, the shifts are cumulative sums of functions from a significantly fluctuating mean latitude curve (see Fig. 15). Thus evidence for the persistence of this phenomenon across the two methods of determining rotating frames is not sufficiently established.

Consequently it is not reasonable to combine the results obtained from one frame system with the results of a totally different system.

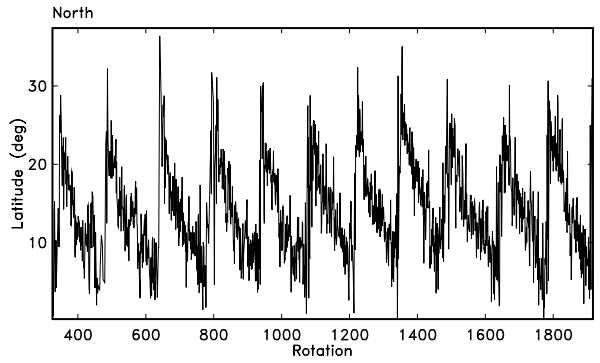

Fig. 15. The mean latitude of sunspots(weighted by sunspot area) against time. The magnitude of the fluctations against the general trend can be seen.

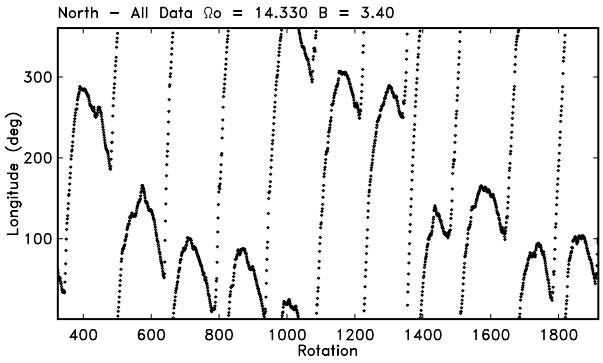

Fig. 16. Particular shifts for a contramoving frame with $\Omega_0 = 14.330$ and $B = 3.40$ folded with module 360°.

5.3. Nonaxisymmetric distributions in fixed velocity frames

It is a major point of the UBP analysis that measures of nonaxisymmetry are low ($\Gamma = 0.02 - 0.03$) for frames with fixed rotation (see Fig. 7 in UBP). In our computations we obtained a relatively high Γ for fixed rotation frames (see Table 1), of the same order as the best values for differentially rotating frames. Since we have demonstrated that the UBP merit function shows rapid fluctuation with respect to changes in the parameter values, it is also very possible that results are sensitive to preprocessing of data. Accordingly we have published on the web the exact data that we used (c.f. section 2.2). We think that in looking for evidence of persistent longitudes it is necessary to examine parameter space very carefully and be completely explicit about all data processing steps used, with publication of data as an aid to other researchers.

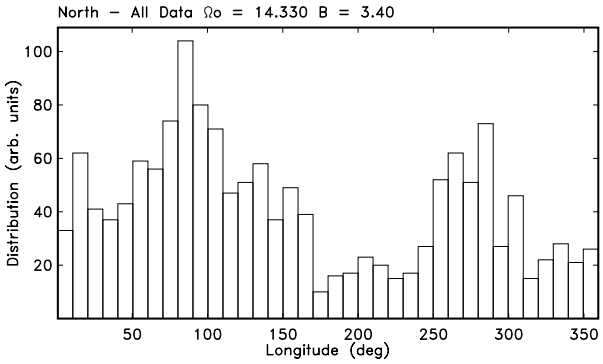

Fig. 17. The marginal distribution (along longitudes) of the frame depicted in Fig. 16.

5.4. The effects of folding phase shifts

In the process of seeking other possible reasons for differences between our computations and those of UBP we folded (by 360°) the shift curves with different parameter values. In Fig. 16 the shift curve for the UBP contramoving frame is depicted. The key features in this plot are the "S"-shaped fragments. For different frame parameters these fragments line up differently. The corresponding marginal distributions in Fig. 17 show that the shifts themselves are not distributed evenly. In Fig. 18 we have depicted how the merit function changes for a fixed value of $B = 3.40$ and changing value of Ω_0. The plot demonstrates that the merit function has a specific wide depression; in the bottom of this depression around Ω_0 values $14.20 - 14.40$ there are deeper minima. Fig. 18 (inlet) reveals that the deepest minimum occurs at $\Omega_0 = 14.316$. The second deepest is at $\Omega_0 = 14.330$. Comparison of Fig. 17 and Fig. 19 shows that the value $\Omega_0 = 14.330$ is *the strongest peak whose shift system has a characteristic double mode distribution*. Just to remind the reader,

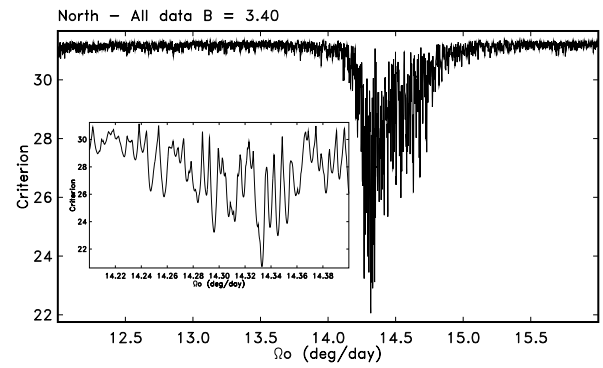

Fig. 18. The merit function computed with longitudes set to zero. There is a strong depression around $\Omega_0 = 14.20 - 14.40$. Enlargement of the depression part is given as inlet.

we *did not use longitudes at all* to compute the last three plots. We can see how sensitive the form of the distribution is to parameter values giving merit function minima of comparable strength.

We draw also attention to the particular value of $\Omega_0 = 14.33$ deg/day, which occurs both as a solution in UBP and as fluctuations in the input data (shift curve) for

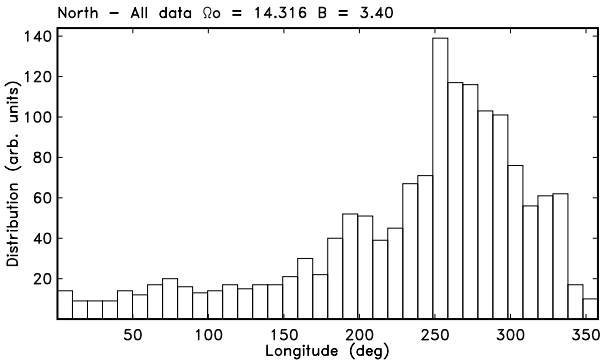

Fig. 19. The marginal distribution for the frame with $\Omega_0 = 14.316$ and $B = 3.40$. (compare with Fig. 17).

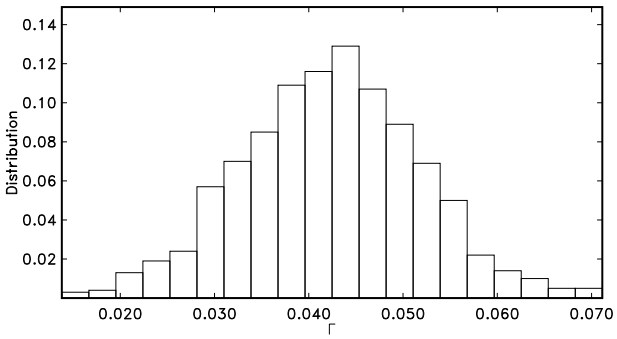

Fig. 20. Distribution of records for fully decorrelated data.

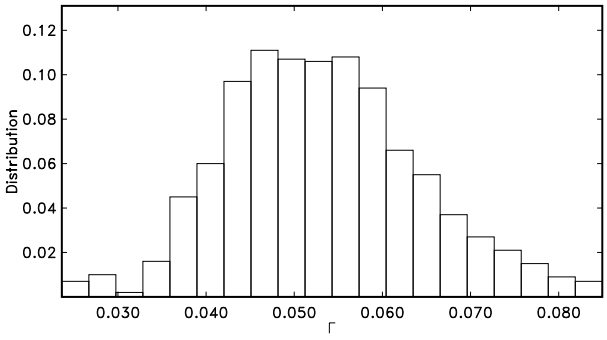

Fig. 21. Distribution of records for short-term correlated data.

the Northern and Southern hemispheres: is there anything peculiar behind this coincidence? The unexpected solution can be found with the help of the previous analysis. To compute minima for the large parameter grid we used certain reparameterization where we divided the frame shift curves into two parts: the linearly rising part and the cyclical part. From the linear part we computed then mean rotation velocity for the frame. For the particular values $B = 3.40$ and $\Omega_0 = 14.330$ this gives $\Omega'_0 = 14.094$. The charming magic of this value reveals itself when we compute first how much it differs from the Carrington siderial value $\Omega_C - \Omega'_0 = 0.090$. From the angular velocity we can compute the corresponding period which occurs to be 10.96 years - closely coinciding with the mean solar sunspot cycle length. The obtained result can also be read out from Fig.1 in BMSU - there are approximately 11 cycles and the range of the shifts is also approximately 11 full rotations.

5.5. Selection of a correct null hypothesis

We now consider the selection of a null hypothesis to check the significance of evidence for persistence in the longitudes of sunspot activity. In UBP the significance of the obtained results was evaluated using a reference (null hypothesis) distribution which was computed using Monte-Carlo type methods. For each Carrington rotation they randomly permuted all the sunspots, i.e., *a new set of random Carrington longitudes* were ascribed to each actually observed sunspot while keeping its area. Then the value of Γ was calculated as described above. They computed the nonaxisymmetry Γ for 5000 sets of such random-phase sunspot occurrences to get a reference distribution. This is a valid procedure for the case when we need to test certain particular longitude distributions against totally random distributions.

However, this analysis does not take into account the fact that we select the best fit solution among number of candidate solutions. Consequently we need to compute the "false alarm probabilities" (see for detailed explanation Scargle 1982). Thus in the Monte-Carlo framework we must compute distributions for "record values". The full scale, full resolution Monte-Carlo computation for full Ω_0,B parameter space is certainly out of our computational capabilities. Fortunately, the general picture becomes evident from a subset of calculations. First we restricted our computations to parameter space slices with fixed parameter $B = 3.40$ and a grid with moderate resolution for Ω_0 - [13.5,15.0,0.01] (Northern hemisphere). Then we performed for 1000 randomized (as in UBP) data sets search for strongest peak in Ω_0 spectrum. For the strongest peak we computed the value for Γ. The corresponding value distribution is depicted in Fig. 20. It is evident that, even for fully decorrelated data, the record values can be quite high. This can be explained by the fact that all data points are not equal - they are weighted by area. The areas differ very significantly (from 0 to 1894 millionths of total area) and the number of effective degrees of freedom to be distributed along longitudes is significantly less than total number of activity elements (18680).

It is known that in the Sun we can observe quite long-lived activity complexes, for instance hot spot systems of solar flares with lifetimes of the order of the solar cycle

length (Bai 1988, 2003). To model this kind of situation we performed an additional test. Instead of full randomization of the longitudes we divided the full observational data into 10 rotation length sections. For each of the 1000 Monte-Carlo runs we added random shifts from the interval $[0, 360]$ to every section. In this way local correlations remained untouched, but long range correlations (if present) were certainly washed out. The record distribution for this experiment is depicted in Fig. 21 and it is to be compared with results in table 1. We see that we can safely treat global minima as the random fluctuations due to the local correlations and the uneven distribution of sunspot areas. Our analysis is conservative - we undersampled along Ω_0 parameter, we used a fixed value of B and we did not seek minima in Γ but in the UBP merit function.

In addition to the above mentioned correlations there is another source of flexibility in the UBP method which results in additional fluctuations. This is due to the reweighting procedure chosen. In the input data set there are some rotations which contain nearly 70 new activity elements and all these get minuscule weights in the method. The weights for the elements which happen during the rotations between the activity cycles, on the other hand, are very powerfully amplified because these rotations are strongly underpopulated (rotations with only a single new event occur reasonably often). As a result, many kinds of distribution may form (see for instance Fig. 14). Instead of amplifying the effect of persistent activity waves the method amplifies random fluctuations.

5.6. Inherent constraints of the data set.

Given the difficulties we have described above we examine the constraints caused by the limited time span of the data set, relative to the solar cycle. The normal comoving flow of the activity indicators can be appropriately measured by such methods. But for activity waves which travel in the opposite direction to solar rotation the evidence can only be quite a weak difference between a low level real physical effect and the fluctuations which result from the statistical nature of the data at hand.

As shown in PTB it is possible to combine a small number of long stretches of data (using appropriate phase corrections) so that their marginal distribution is almost entirely an artefact of the method of analysis.

The inherent (for such an analysis) phase ambiguity is a strong constraint which can be overcome only by using much longer (in time) data sets. The current time extent of the sunspot database covers only a small number of correlation length size subparts and this results in a high level of random fluctuations. We do not deal here with 1600 independent rotations but with a significantly lower amount of activity complexes.

6. Conclusions

In the recent papers BU, UBP and BMSU the authors claim that, hidden in the sunspot distribution, there are two persistent active longitudes which migrate according to a certain differential rotation law. After presenting a critique of the BU results in the earlier paper (PTB), here we have tried to check the results obtained in UBP and the data analysis part of BMSU. Our results can be summarized as follows:

- The contramoving frames constructed by BU differ significantly from the frames found using mathematical optimization techniques in UBP and BMSU. In the first case the frame does approximately 28 extra rotations (compared with the Carrington frame) and in the new papers the number of extra rotations is around 10-11 for the Northern hemisphere and 13-14 for the Southern hemisphere. Consequently the claim in UBP that the new analysis confirms the results obtained in the previous study is not well founded.
- In the two latest papers authors re-iterate the claim presented in BU of the presence of the flip-flop effect with a mean period of 3.7 years. This result was obtained from (and now presumably incorrect) analysis in the first paper (BU).
- Our analysis demonstrated that even for fixed angular velocity contramoving frames it is quite easy to get particular longitude distributions with relatively high values of nonaxisymmetry. This result is quite robust and does not depend on the particular implementation of the UBP method (smoothing of the shift curve, sampling rates in the parameter space etc.). Consequently all the claims in UBP about $\Gamma = 0.02 - 0.03$ level fluctuations in the case of $B = 0$ are incorrect. The parameter space is full of parameter combinations which can give a rather high values for nonaxisymmetry.
- Our re-implemantion of the UBP method gave fundamentally different results from those of the original authors. We can only conjecture about the possible reasons for the discrepancies. The pre- or postselection of data points, parameter undersampling in search procedures, incorrect phase reduction etc. - these all can be considered as possible sources of differences.
- From inspection of the strongly fluctuating merit function curves and additional Monte-Carlo type computations for parameter space slices, we conclude that the frames obtained from the optimization procedure are pure fluctuations.
- We found that the parameter values obtained as results in UBP can be seen already in the distributions connected to the frame shift curve itself (which does not depend on longitudes of sunspots at all).
- Our analysis does not indicate that short-lived features concentrated in certain longitude are totally missing in the sunspot distribution, even though evidence for century scale persistent active longitudes can not be found. The simple cell-counting method investigated

here merely as a demonstration tool may well be used to estimate real coherence times of these structures.
– Whichever method used, the preferred solutions occurred at positive/negative values of the differential rotation parameter B in the comoving/contramoving frame systems, respectively, i.e. the frames had a tendency to follow a solar-type differential rotation pattern.

From this we conclude that the results obtained in BU, UBP and BMSU (data analysis part) are inconsistent, and evidence for well established persistent activity migration is still lacking. In other words we are inclined to think that the enigmatic face of the Sun is still hidden and that the patterns which the authors of the three papers saw have a human origin.

Acknowledgements. We are thankful to anonymous referee and A. Brandenburg for helpful comments on the manuscript and I.G. Usoskin for additional comments about data processing procedures used in the UBP paper. Part of this work was supported by the Estonian Science Foundation grant No. 6813 and Academy of Finland grant No. 1112020.

References

Bai T., 1988, ApJ, 328, 860
Bai T., 2003, ApJ, 585, 1114
Berdyugina S.V., Moss D., Sokoloff D., Usoskin I. G., 2006, A&A, 445, 703 (BMSU)
Berdyugina S.V., Usoskin I.G., 2003, A&A, 1121 (BU)
Brandenburg A., Tuominen I., Krause F., Meinel R., Moss D., 1989, A&A, 213, 411
Jetsu L., Pelt J., Tuominen I., 1993, A&A, 278, 449
Krause F., Meinel R. 1988, Geophys. Astrophys. Fluid Dynamics 43, 95
Krause F., Rädler K.-H. 1980, Mean-field magnetohydrodynamics and dynamo theory, Akademie-Verlag Berlin
Moss D., Tuominen I., Brandenburg A., 1991, A&A, 245, 129
Parker E.N., 1955, ApJ, 122, 293
Pelt J., Tuominen I., Brooke J., 2005, A&A, 429, 1093 (PTB)
Pulkkinen P., Tuominen I., 1998, A&A, 332, 748
Rädler K.-H., Wiedemann E., Meinel R., Brandenburg A., Tuominen I., 1990, A&A, 239, 413
Scargle J.D., 1982, ApJ, 263, 835
Schou, J., Antia, H. M., Basu, S. et al., 1998, ApJ, 505, 390
Steenbeck M., Krause F. 1969, AN 291, 49
Stenflo J-O., in The Sun and Cool Stars: activity, magnetism, dynamos, Proc. of IAU Colloquium 130, Helsinki 1990, eds. I.Tuominen, D.Moss, G. Rüdiger, Lecture Notes in Physics, Springer-Verlag, Heidelberg, 1991, p. 193
Tuominen I., Virtanen H., 1987, in the Internal Solar Angular Velocity, eds. B.R. Durney and S. Sofia, D.Reidel, 83
Tuominen I., Berdygina S.V., Korpi M.J., Rönty T.,1999, in Stellar Dynamos: nonlinearity and chaotic flows, eds. M. Nunez and A. Ferriz-Mas, ASP Coference series Vol 178, p. 195
Tuominen I., Berdyugina S.V., Korpi M.J., 2002, AN, 323, 367
Usoskin I.G., 2005, private communication
Usoskin I.G., Berdyugina S.V., Poutanen J., 2005, A&A, 441, 347 (UBP)